Journal of Chromatography, 149 (1978) 43–70

CHROM. 10,727

BAND SPREADING IN LIQUID CHROMATOGRAPHY

GENERAL PLATE HEIGHT EQUATION AND A METHOD FOR THE EVALUATION OF THE INDIVIDUAL PLATE HEIGHT CONTRIBUTIONS

CSABA HORVÁTH and HUNG-JYE LIN

Chemical Engineering Group, Department of Engineering and Applied Science, Yale University, New Haven, Conn. 06520 (U.S.A.)

SUMMARY

A general plate height equation has been derived to express the effect of axial dispersion in the interstitial space, mass transfer resistances at the boundary and in the interior of porous stationary phase particles, and kinetic resistances associated with the reversible binding of eluite by the stationary phase. The last process is assumed to obey a simple kinetic law for a single-step reaction. In the case of a given chromatographic run with a sample whose components have commensurate diffusivities and rate constants for binding, the general plate height equation can be rearranged to yield for the dependence of the effective plate height, H_{eff}, on the distribution ratio, k', the equation $H_{eff} = a + bk'^{-1} + ck'^{-2}$. From the parameters of this equation, the plate height contributions of axial dispersion, kinetic resistances and extra-column band spreading can be evaluated, provided that the plate height contribution arising from diffusion resistances can be calculated independently. The use of this approach is appropriate if the plot of peak width against the distribution ratio is linear at sufficiently high k' values. Plate height increments have been evaluated from experimental data obtained with various microparticulate columns under different conditions. The results show the contribution of the individual physico-chemical phenomena to the plate heights measured in a given chromatographic system. The effect of kinetic resistances on the performance of microparticulate columns has been found to be significant. Thus, a lower practical limit for the particle size in high-performance liquid chromatography may be imposed by the slow kinetics of eluite–stationary phase interactions as well.

INTRODUCTION

The increasing use of high-performance liquid chromatography in analysis of non-volatile substances and the availability of precision instrumentation for collecting accurate data have renewed the interest in the analysis of the physico-chemical phenomena underlying the chromatographic process.

Whereas the general theoretical basis of chromatography is well established[1], the widespread use of novel chromatographic systems necessitates further investiga-

tions of the particular equilibrium and transport phenomena which govern retention and band spreading in such systems. The salient features of columns employed in modern liquid chromatography for the separation of sample components that have complex molecular structures are the relatively small particle size of the packing and the chemically bonded nature of the stationary phase proper. Recent studies from our laboratory have been focused on the thermodynamic aspects of retention in reversed-phase chromatography[2] and on the band spreading of non-sorbed tracers in packed columns[3]. This paper considers the factors that affect band spreading of retarded eluites and draws attention to the role of kinetic phenomena associated with the reversible binding of the eluites at the surface of the stationary phase.

THEORETICAL

General plate height equation

The reduced plate height, h, of a non-sorbed tracer in a column packed with porous spherical particles is given[3] by the following expression:

$$h = \frac{2\gamma}{\nu} + \frac{2\lambda}{1 + \omega\nu^{-1/3}} + \frac{\kappa k_0^2}{(1 + k_0)^2} \cdot \nu^{2/3} + \frac{\theta k_0}{30\,(1 + k_0)^2} \cdot \nu \qquad (1)$$

where ν is the reduced interstitial velocity of the mobile phase, γ, λ, ω and κ are structural parameters of the column packing, θ is the tortuosity factor for the porous particles and k_0 is the ratio of the intraparticulate void volume, which is explored by the tracer molecules, to the interstitial void space in the column. The reduced velocity, ν, is given by $d_p u_e / D_m$ where d_p, u_e and D_m are the particle diameter, the interstitial mobile phase velocity and the diffusivity of the tracer in the bulk mobile phase, respectively. The value of k_0 is given by $\varepsilon_i(1-\varepsilon_e)/\varepsilon_e$, where ε_i and ε_e are the appropriate intraparticular and interstitial porosities, respectively. The reduced plate height is defined by H/d_p, where H is the height equivalent to a theoretical plate, *i.e.*, the ratio of the second moment to the first moment of the concentration distribution represented by the chromatographic peak when both moments are expressed in length units.

The terms of eqn. 1 express the plate height contributions which arise from longitudinal molecular diffusion, "eddy" dispersion, the resistance to mass transfer at the particle boundary and from intraparticulate diffusion resistance.

In order to describe the band spreading of a retarded eluite, the previous model has to be extended to account for the interaction of the eluite molecules with the stationary phase. We assume that the reversible binding of the eluite, E, to the active sites or covalently bound ligands, L, at the surface of the stationary phase can be expressed by the simple process

$$\mathrm{E} + \mathrm{L} \underset{k_d}{\overset{k_a}{\rightleftharpoons}} \mathrm{EL} \qquad (2)$$

Denoting the surface concentration of the bound eluite, *i.e.*, that of the complex EL, by c_s, the concentration of the free eluite in the mobile phase by c_m and the surface

concentration of all ligands or active sites accessible to eluite molecules by Λ, we can express the thermodynamic equilibrium constant, K, for the binding process as

$$K = c_s/(\Lambda - c_s)c_m \tag{3}$$

At low eluite concentrations, only a negligibly small fraction of the ligands complexes with the eluite so that $\Lambda - c_s \approx \Lambda$. In the following treatment we assume that this condition of linear chromatography holds and no secondary equilibria are involved in the chromatographic process. The equilibrium constant can also be expressed by the rate constants k_a and k_d for the association and the dissociation processes, respectively, as

$$K = k_a/k_d \tag{4}$$

The mass distribution ratio, k', for the eluite in the column is related to the equilibrium and rate constants by the equation

$$k' = \varphi K = \varphi k_a/k_d \tag{5}$$

where φ is the so-called phase ratio. In our case, φ is given by the concentration of the accessible ligands or active sites expressed with the volume of the mobile phase in the column. It can be shown that

$$\varphi = \frac{k_0 S_p \Lambda}{(1 + k_0) V_p \varepsilon_i} \tag{6}$$

where S_p is the total surface area of the stationary phase particles that is accessible to the eluite molecules and V_p is the volume of the particles.

The mass balance for the eluite in the interstitial space of the column is given by the equation

$$\frac{\partial c_{m,e}}{\partial t} + u_e \cdot \frac{\partial c_{m,e}}{\partial z} = \mathscr{D} \cdot \frac{\partial^2 c_{m,e}}{\partial z^2} - \frac{k_e S_{p,e}}{V_p} \cdot \frac{(1 - \varepsilon_e)}{\varepsilon_e} \cdot (c_{m,e} - c_{m,s}) \tag{7a}$$

with the initial and boundary conditions

$$c_{m,s} = 0 \qquad \text{at } t = 0 \tag{7b}$$

$$c_{m,e} = C_m \delta(t) \qquad \text{at } z = 0 \tag{7c}$$

$$c_{m,e} = 0 \qquad \text{at } z > 0 \text{ and } t = 0 \tag{7d}$$

In eqns. 7a–7d $c_{m,e}$ denotes the eluite concentration in the bulk mobile phase; u_e is the interstitial fluid velocity, t is time, z is the axial position in the column, $\mathscr{D}$ is the axial dispersion coefficient for the eluite in the interstitial space, k_e is the mass transfer coefficient for the eluite at the grain boundary, $c_{m,s}$ is the eluite concentration at the outer surface of the particles and $S_{p,e}$ is the external surface area of the stationary phase particles. The eluite concentration at the column inlet is given by a delta function.

According to our previous treatment[3], the axial dispersion coefficient and the mass transfer coefficient can be expressed as

$$\mathscr{D} = D_m + \frac{\lambda\, d_p\, u_e}{1 + \omega\nu^{-1/3}} \tag{8}$$

and

$$k_e = \Omega D_m \nu^{1/3}/d_p \tag{9}$$

where D_m is the diffusivity of the eluite in the bulk mobile phase and Ω is related to the column parameter κ by

$$\kappa = \frac{\varepsilon_e}{3\Omega\,(1 - \varepsilon_e)} \tag{10}$$

The transient penetration of the eluite into the porous spherical particles of the stationary phase is expressed by the equation

$$\frac{\partial c_{m,i}\,(r)\,\varepsilon_i}{\partial t} + \frac{\partial c_s\,(r)}{\partial t}\cdot\frac{S_p}{V_p} = D_{m,i}\cdot\frac{1}{r^2}\cdot\frac{\partial}{\partial r^2}\left[r^2\,\frac{\partial c_{m,i}\,(r)}{\partial r}\right] \tag{11a}$$

with the boundary conditions

$$\frac{\partial c_{m,i}\,(r)}{\partial r} = 0 \qquad \text{at } r = 0 \tag{11b}$$

$$c_{m,i}(d_p/2) = c_{m,s} \tag{11c}$$

All concentrations in eqns. 7a and 11a are functions of both time and axial position in the column. In eqn. 11a, $c_{m,i}$ is the eluite concentration in the stagnant mobile phase inside the particle and c_s is the surface concentration of the bound solute (complex), both are also functions of the radial position, r, in the particle. $D_{m,i}$ is the effective diffusivity of the eluite in the porous particle and is related to D_m by

$$D_{m,i} = D_m\varepsilon_i/\theta \tag{11d}$$

where θ is the tortuosity factor. The transport processes represented in eqns. 7a and 11a are illustrated schematically in Fig. 1.

The kinetics of the reversible binding of the eluite to the ligand or active sites at the stationary phase surface inside the particles may also affect the transfer of the eluite. Therefore, we do not assume instantaneous equilibration in the pores as is customary[4], but relate the local surface concentration of the eluite in the stagnant mobile phase by a kinetic expression for the overall binding process which is illustrated schematically in Fig. 2. Recognizing that the kinetic phenomena involved may be very complex, as a first approximation we assume that the concentration change of the bound eluite follows the simple kinetic law

$$\frac{\partial c_s\,(r)}{\partial t} = k_a\, c_{m,i}\,(r)\,A - k_d\, c_s\,(r) \tag{12}$$

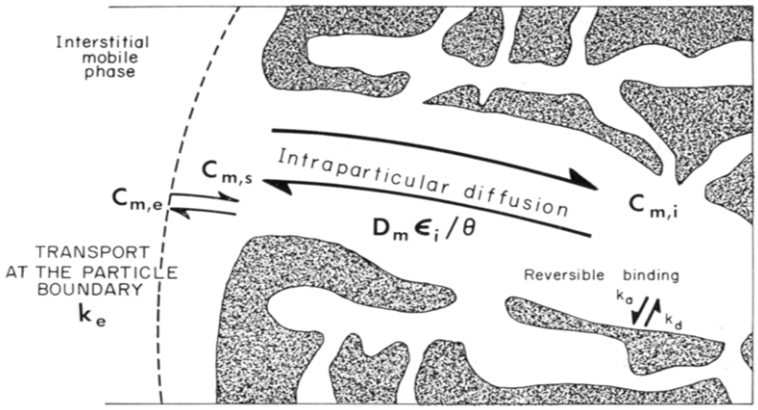

Fig. 1. Schematic illustration of eluite diffusion into the stationary phase particles.

and the ligand or active site concentration, A, is constant. The initial conditions for eqns. 11a and 12 are given by

$$c_s(r) = 0 \text{ and } c_{m,i}(r) = 0 \qquad \text{at } t = 0 \tag{13}$$

The mathematical model represented by the above t of partial differential equations describes the entire chromatographic process in the column. The equations can be solved by a variety of methods to obtain the overall transfer function, which can be used to evaluate the moments of the concentration distribution of the eluite after passing through a column of length L. The distribution ratio, k', is evaluated from the first moment of the eluite and that of a tracer, which is given by $u_e (1 + k_0)/L$. The second central moment normalized to the first moment of the eluite and multiplied by

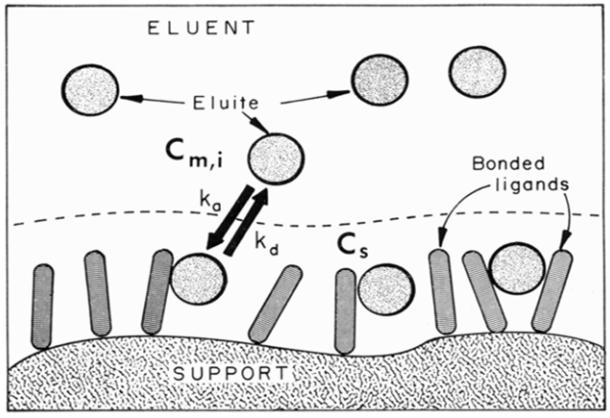

Fig. 2. Schematic illustration of the reversible binding of the eluite to the covalently attached ligands at the stationary phase surface.

the column length yields the plate height, which is expressed by the following dimensionless equation:

$$h = \frac{2\gamma}{\nu} + \frac{2\lambda}{1+\omega\nu^{-1/3}} + \frac{\kappa(k_0+k'+k_0k')^2}{(1+k_0)^2(1+k')^2}\cdot\nu^{2/3} + \frac{\theta(k_0+k'+k_0k')^2}{30k_0(1+k_0)^2(1+k')^2}\cdot\nu + \\ + \frac{2k'D_m}{(1+k_0)(1+k')^2d_p^2k_d}\cdot\nu \qquad (14)$$

Eqn. 14 is believed to express adequately the reduced plate height as a function of the system parameters and the reduced velocity over a wide range of ν, provided that secondary equilibria and kinetic phenomena in the mobile phase, column end effects and a non-uniform radial temperature profile due to viscous dissipation do not cause a departure from the model and the overall binding kinetics can be represented by eqn. 12.

Plate height increments

Eqn. 14 can be written as

$$h = h_{\text{disp.}} + h_{e.\text{diff.}} + h_{i.\text{diff.}} + h_{\text{kin.}} \qquad (15)$$

and the terms on the right-hand side of eqns. 14 and 15 represent the individual plate height contributions arising from the different processes that take place independently in the column.

The term $h_{\text{disp.}}$ expresses the plate height increment due to axial dispersion of the eluite in the interstitial space. It is believed to be unaffected by the retention of the eluite on the stationary phase. Its dimensional expression, $H_{\text{disp.}}$, is given by

$$H_{\text{disp.}} = h_{\text{disp.}}\,d_p = \frac{2\gamma D_m}{u_e} + \frac{2\lambda\,d_p\,u_e^{1/3}}{u_e^{1/3}+\omega\,(D_m/d_p)^{1/3}} \qquad (16)$$

The first term on the right-hand side of eqn. 16 is due to longitudinal molecular diffusion whereas the second term expresses the combined effect of the flow velocity field and diffusion in the interstitial space. The latter expression is referred to as "eddy" dispersion and is similar to those given by Giddings' coupling theory[1] and by Huber[5]. The structural parameters of the column packing, λ and ω, can significantly vary from column to column as their values are determined by the properties of the column material, tube dimensions and material as well as by the packing procedure. Consequently, these parameters have to be evaluated experimentally for a given column.

The plate height increment $h_{e.\text{diff.}}$ is related to the "film" resistance at the particle boundary and its dimensional form, $H_{e.\text{diff.}}$, is given by

$$H_{e.\text{diff.}} = h_{e.\text{diff.}}\,d_p = \frac{\kappa\,(k_0+k'+k_0\,k')^2\,d_p^{5/3}\,u_e^{2/3}}{(1+k_0)^2\,(1+k')^2\,D_m^{2/3}} \qquad (17)$$

The magnitude of the packing structure parameter, κ, has been discussed earlier[3]. For

columns that have an interstitial porosity, ε_e, of about 0.4, which is typical for random packing of spheroidal particles, the value of κ is *ca.* 1/15.

The intraparticular diffusion resistance to mass transfer is represented by the term $h_{i.\mathrm{diff.}}$. For spherical particles, the dimensional form of this term, $H_{i.\mathrm{diff.}}$, is given by

$$H_{i.\mathrm{diff.}} = h_{i.\mathrm{diff.}}\, d_p = \frac{\theta\,(k_0 + k' + k_0\,k')^2\, d_p^{\,2}\, u_e}{30\, D_m\, k_0\,(1 + k_0)^2\,(1 + k')^2} \tag{18}$$

The expression in eqn. 18 is the same as those in the literature that were derived by using other approaches[4].

The kinetic resistance for eluite binding gives rise to $h_{\mathrm{kin.}}$, which can be expressed by either k_a or k_d. The dimensional form of this term, $H_{\mathrm{kin.}}$, is given by

$$H_{\mathrm{kin.}} = h_{\mathrm{kin.}}\, d_p = \frac{2\,k'\,u_e}{(1 + k_0)\,(1 + k')^2\,k_d} = \frac{2\,k'^2\,u_e}{(1 + k_0)\,(1 + k')^2\,\varphi\,k_a} \tag{19}$$

The mechanism and kinetics of the eluite binding and dissociation processes at the stationary phase surface are largely unexplored in the case of such complex molecules that are commonly separated in liquid chromatography. Consequently, we cannot estimate the magnitude of the plate height contribution due to the slowness of the binding kinetics. On the other hand, the expressions for $H_{e.\mathrm{diff.}}$ and $H_{i.\mathrm{diff.}}$ allow the calculation of the plate height contributions which arise from resistance to mass transfer. Therefore, further insight could be gained into the chromatographic process if $h_{\mathrm{kin.}}$ as well as the phenomenological rate constants k_a and k_d could be evaluated experimentally.

Simplified plate height equations

Eqn. 14 can be written in the form

$$h = \frac{A}{\nu} + \frac{2\lambda}{1 + \omega\,\nu^{-1/3}} + C\,\nu^{2/3} + D\,\nu \tag{20}$$

At sufficiently low reduced velocities, *i.e.*, $\nu^{1/3} \ll \omega$, eqn. 20 reduces to the approximation

$$h \approx \frac{A}{\nu} + 2\cdot\frac{\lambda}{\omega}\cdot\nu^{1/3} + \left(C - \frac{2\lambda}{\omega^2}\right)\nu^{2/3} + \left(D + \frac{2\lambda}{\omega^3}\right)\nu \tag{21}$$

In most practical situations, $(C - 2\lambda/\omega^2)\nu^{2/3}$ is expected to be smaller than the other terms and $D \gg 2\lambda/\omega^3$. Therefore, eqn. 21 can be further simplified to

$$h \approx \frac{A}{\nu} + B\,\nu^{1/3} + D\,\nu \tag{22}$$

where $B = 2\lambda/\omega$.

Eqn. 22 has the same form as the empirical equation proposed by Done *et al.*[6] for analysing chromatographic data obtained at relatively low reduced velocities

which are of practical interest. Thus, the present treatment gives theoretical support to the so-called Knox equation which is widely used for curve fitting in liquid chromatography.

At relatively high reduced velocities, *i.e.*, $\nu^{1/3} \gg \omega$, eqn. 20 reduces to the simple form

$$h \approx 2\lambda + D\nu \tag{23}$$

which predicts a linear dependence of the plate height on the velocity. Such behavior has indeed been observed. For instance, Endele and Halász[7] fitted their data by using a simple linear relationship such as eqn. 23.

Dependence of the plate height on the distribution ratio

As shown in this section, when closely related substances are separated in a single chromatographic run under isocratic and isothermal conditions, the plate height of the individual eluites can be expressed as a function of their distribution ratio, provided that D_m, k_0, and k_a are the same for all components. Whereas these conditions do not apply to mixtures in general, it is possible to select sample components so that their diffusivities and molecular dimensions, which affect the value of k_0, are nearly the same. In such a mixture we may assume that the k_a values do not vary significantly.

At this point, it should also be mentioned that the recorded peak variance is often affected by the magnitude of extra-column band spreading measured by its variance, σ_E^2. An extra-column "plate height contribution", $h_{e.c.}$, can be defined as

$$h_{e.c.} = \left[\frac{\sigma_E}{t_0 (1 + k')}\right]^2 \frac{L}{d_p} \tag{24}$$

where t_0 is the retention time of a non-sorbed solute that has the same molecular dimensions as the other sample components.

Knowing that the additivity of variances holds for the extra- and intra-column plate height contributions and combining $h_{e.diff.}$ and $h_{i.diff.}$ into a single term, $h_{diff.}$, we can re-write eqn. 15 with the extra-column plate height contribution as

$$h = h_{e.c.} + h_{disp.} + h_{diff.} + h_{kin.} \tag{25}$$

When D_m, k_0, and k_a are practically invariant for all sample components in a chromatographic run, the rearrangement of eqn. 25 yields the following equation[8] for the effective reduced plate height, $h_{eff.}$:

$$h_{eff} = h\left(\frac{1 + k'}{k'}\right)^2 = a + \frac{2b}{k'} + \frac{c}{k'^2} \tag{26}$$

The parameter a in eqn. 26 is given by

$$a = h_{disp.} + h^0_{diff.}\left(\frac{1 + k_0}{k_0}\right)^2 + h_{kin.}\left(\frac{1 + k'}{k'}\right)^2 \tag{27}$$

where $h^0_{\text{diff.}}$ is the reduced plate height contribution arising from the mass transfer resistance for a non-sorbed tracer that has the same molecular size and diffusivity as the other sample components and can be calculated from the expression

$$h^0_{\text{diff.}} = \frac{1}{15}\left(\frac{v}{k_0} + v^{2/3}\right)\left(\frac{k_0}{1 + k_0}\right)^2 \tag{28}$$

assuming random packing of spherical particles, *i.e.*, $\varepsilon_e = 0.4$, and that $\theta \approx 2$. The reduced velocity is calculated from the particle diameter, the molecular diffusivity of the eluites and the interstitial velocity. The magnitude of k_0 is calculated from ε_i and ε_e or evaluated from the chromatographic velocity of a suitable tracer and the interstitial velocity[3]. The parameter b has the form

$$b = h_{\text{disp.}} + h^0_{\text{diff.}}\left(\frac{1 + k_0}{k_0}\right) \tag{29}$$

The parameter c is given by

$$c = h^0_{\text{e.c.}} + h_{\text{disp.}} + h^0_{\text{diff.}} \tag{30}$$

where $h^0_{\text{e.c.}}$ is the extra-column plate height contribution of the non-sorbed tracer. It can be seen that c is the reduced plate height measured for a non-sorbed tracer (*cf.*, eqn. 1) and includes the effect of extra-column band spreading.

As shown later, eqn. 26 can be used to evaluate $h_{\text{e.c.}}$, $h_{\text{disp.}}$ and $h_{\text{kin.}}$ from data obtained in a single chromatographic run, provided that $h^0_{\text{diff.}}$ can be accurately calculated by using eqn. 28.

Quasi-linear dependence of peak width on the distribution ratio

The width of a chromatographic peak, σ, in time units can be expressed as

$$\sigma = k' t_0 \sqrt{\frac{h_{\text{eff.}} d_p}{L}} \tag{31}$$

Substituting the square root of the right-hand side of eqn. 26 into eqn. 31, we obtain an analytical expression for the peak width as a function of the distribution ratio. This relationship is illustrated schematically in Fig. 3. The graph is non-linear at low k' values but approaches a straight line at sufficiently large values of the distribution ratio. The intercept of this straight line on the ordinate line is σ_{III} and the intercept of the curve calculated from the analytical expression with $h_{\text{e.c.}} = 0$ is given by σ_{II}. The two intercepts are different because the difference of the corresponding two variances given by the following equation is small but not equal to zero:

$$\sigma^2_{\text{II}} - \sigma^2_{\text{III}} = \frac{d_p t_0^2}{L}\left\{(h_{\text{disp.}} + h^0_{\text{diff.}}) - \frac{\left[h_{\text{disp.}} + h^0_{\text{diff.}} \cdot \frac{(1 + k_0)}{k_0}\right]^2}{\left[h_{\text{disp.}} + h^0_{\text{disp.}}\left(\frac{1 + k_0}{k_0}\right)^2 + h_{\text{kin.}}\left(\frac{1 + k'}{k'}\right)^2\right]}\right\} \tag{32}$$

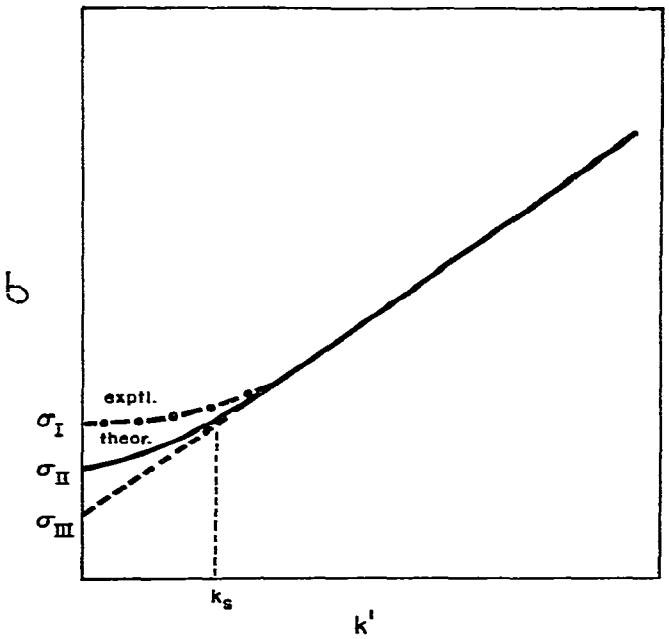

Fig. 3. Graph illustrating the plot of band width, σ, against the distribution ratio, k'. The intercepts σ_{III}, σ_{II}, and σ_I represent those of the asymptotic straight line, the theoretical value, and an experimental curve obtained with appreciable extra-column band spreading, respectively. The distribution ratio at which deviation of the theoretical curve from the asymptotic straight line is 5% is denoted by k_s.

The magnitude of the variance difference given in eqn. 32 relative to σ_{II}^2 is shown as a function of the reduced velocity with the particle diameter as the parameter in Fig. 4. The chromatographic parameters used for calculating the results are typical for those encountered in reversed-phase chromatography. It can be seen that $\Delta\sigma^2 = \sigma_{II}^2 - \sigma_{III}^2$ can exceed 70% of σ_{III}^2, which is the square of the ordinate intercept of the asymptotic straight line in Fig. 3.

With increasing k', however, the deviation from linearity rapidly attenuates. In order to illustrate the dependence of the deviation on the system parameters, we define k_s' as the distribution ratio above which the theoretical departure of σ from that calculated by the expression

$$\sigma = k'\sqrt{a} + \frac{b}{\sqrt{a}} \tag{33}$$

is less than 5%. Fig. 5 shows k_s' values calculated as a function of the reduced velocity for 5- and 10-μm particles with other parameters typically found in liquid chromatography. It can be seen that under conditions typical of high-performance liquid chromatography, k_s' is less than unity and does not depend much on the particle diameter at sufficiently high reduced velocities. Nevertheless, deviation from the "ideal" behavior can be observed when the extra-column band spreading contributes significantly to the bandwidth, as illustrated by the dash-dot line in Fig. 3. Consequent-

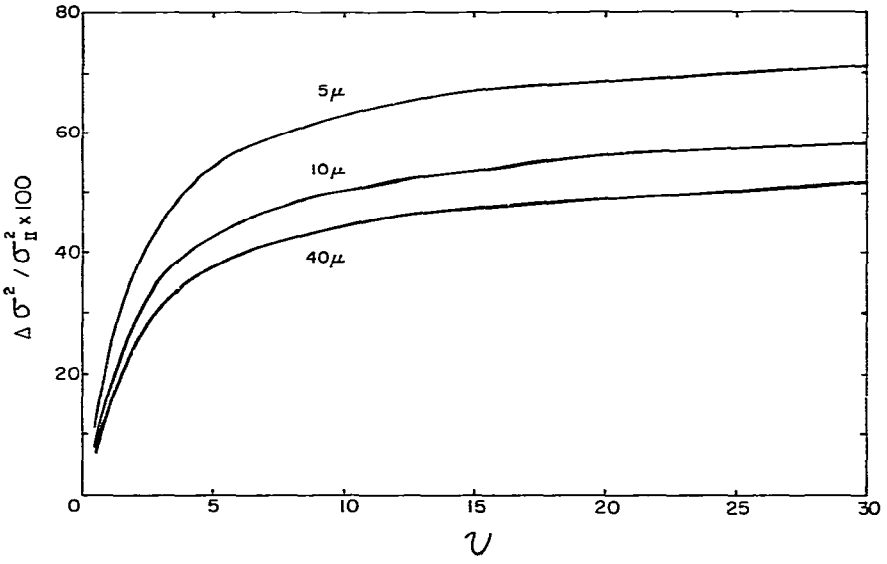

Fig. 4. Graph illustrating the relative magnitude of the variance difference given in eqn. 32 as a function of the reduced velocity with the particle diameter as the parameter under conditions typical for reversed-phase chromatography. The ordinate shows the difference of the variances σ_{II}^2 and σ_{III}^2 at $k' = 0$ (see Fig. 3 for the meaning of σ_{II} and σ_{III}) as a percentage of σ_{II}^2.

ly, extra-column effects can result in significantly higher experimental k_s values than the theoretical values calculated without considering extra-column band spreading.

However, when the chromatogram is obtained under carefully controlled conditions, plots of the bandwidth against the distribution ratio or some other measure of retention can yield straight lines in a practical range of the k' values, provided that the diffusivities and the k_a values of the sample components, if kinetic resistances are significant, are nearly the same. Consequently, such plots are eminently suitable

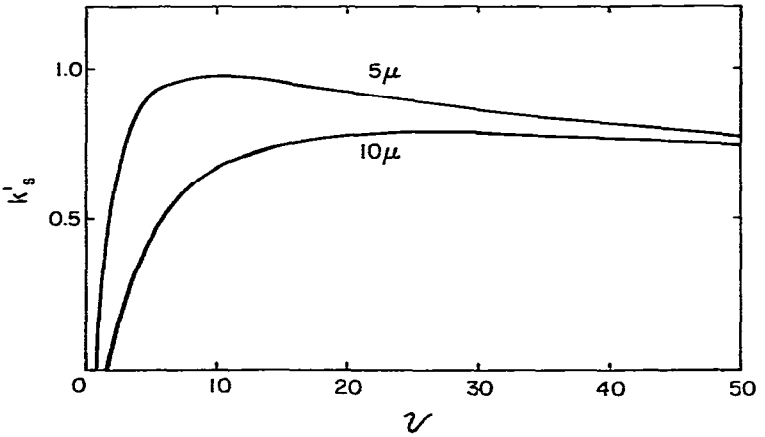

Fig. 5. Plot of k'_s against the reduced velocity for 5- and 10-μm particles. Data typical for reversed-phase chromatography with predominantly aqueous eluents were used in the calculations.

to check whether the requirements for eqn. 26 to be valid under a given set of experimental conditions are fulfilled.

Evaluation of the plate height contributions

In order to use eqn. 26 for the evaluation of the individual plate height contributions, a suitable mixture has to be prepared so that the k_0 values for all components and D_m and k_a values for the retained components are about the same. After chromatograms under controlled conditions have been obtained, the fulfillment of this requirement can be tested by the linearity of the σ *versus* k' plot at sufficiently high k' values. From the retention time of the non-sorbed tracer component, t_0, the column length, L, and ε_0, the value of k_0 can be calculated by

$$k_0 = \frac{t_0 - t_e}{t_e} = \frac{t_0 u_e - L}{L} \tag{34}$$

where t_e is the retention time of a tracer which does not enter the intraparticular space[3] and u_e is obtained from the experimentally measured volumetric flow-rate, F, by $u_e = F/A\varepsilon_e$, where A is the cross-section of the empty column. The molecular diffusivities can be obtained from the literature by using the Wilke–Chang equation[9] or other correlations. With these data, the value of $h_{\text{diff.}}$ can be calculated from eqn. 28 for columns packed with spherical particles of known diameter.

The value of the distribution ratio is calculated from the chromatogram by

$$k' = \frac{t_R - t_0}{t_0} \tag{35}$$

where t_R is the retention time of the eluite. The reduced effective plate height is calculated from the standard deviation of the chromatographic peak, σ, measured by one of the conventional methods[8], by the relationship

$$h_{\text{eff.}} = \left(\frac{\sigma}{t_0 k'}\right)^2 \frac{L}{d_p} \tag{36}$$

The parameters a, b and c in eqn. 26 are obtained by regression analysis. With the estimated value of $h^0_{\text{diff.}}$ and the parameters a, b and c, the extra-column "plate height" contribution, $h_{\text{e.c.}}$, is calculated by

$$h_{\text{e.c.}} = \left[\frac{\sigma_E}{t_0 (1 + k')}\right]^2 \frac{L}{d_p} = \frac{(c - b + h^0_{\text{diff.}})}{(1 + k')^2} \tag{37}$$

The magnitude of the plate height contribution of axial dispersion is obtained by

$$h_{\text{disp.}} = b - (1 + k_0)\, h^0_{\text{diff.}} \tag{38}$$

and the plate height increment associated with kinetic resistances is calculated by using the relationship

$$h_{\text{kin.}} = \left(\frac{k'}{1 + k'}\right)^2 \left[a - b - \frac{(1 + k_0)}{k_0} \cdot h^0_{\text{diff.}}\right] \tag{39}$$

Thus, eqns. 37–39 allow us to evaluate, at least in principle, the three plate height contributions, $h_{e.c.}$, $h_{disp.}$ and $h_{kin.}$, from a single chromatographic run. It has been assumed that the theory has been developed adequately for calculating the plate height increment due to mass transfer resistances, $h_{diff.}$, by the relationship

$$h_{diff.} = h^0_{diff.} \left[\frac{(k_0 + k' + k_0 k')}{k_0 (1 + k')}\right]^2 \tag{40}$$

Eqn. 40 can also be expressed by Golay's[10] "virtual k", k_v, given by

$$k_v = k_0 + k' + k_0 k'$$

as

$$h_{diff.} = h^0_{diff.} \left[\frac{(1 + k_0) k_v}{k_0 (1 + k_v)}\right]^2 \tag{42}$$

By calculating the plate height contributions from eqns. 37–40, we can evaluate all terms in eqn. 25 for each solute under the chromatographic conditions employed and establish their relative importance. The kinetic constant k_d or the value of φk_a can readily be obtained from the magnitude of the corresponding $h_{kin.}$ and k' values. When experiments are carried out over a sufficiently wide range of reduced velocities, this approach may be useful in calculating the structural parameters of the column packing, γ, λ and ω, from $h_{disp.}$ measured at different flow velocities.

EXPERIMENTAL

A Perkin-Elmer (Norwalk, Conn., U.S.A.) Model 601 liquid chromatograph with a Rheodyne (Berkeley, Calif., U.S.A.) Model 7010 sampling valve and a Perkin-Elmer Model 250A fixed wavelength UV detector was used. The extra-column dead space was different in each experiment. The temperature of the eluent feed and the column was controlled by circulating water through appropriate jacketing from a Model K2R-D (Messgeräte Werk Lauda, Lauda, G.F.R.) constant-temperature bath. Most measurements were made at 23°; for evaluation of the temperature dependence of the plate height and distribution ratio, the column temperature was varied between 10 and 50°.

Both commercial and home-made columns were used. A Chromegasorb R column (30 × 0.46 cm) packed with irregularly shaped 5-μm silica gel of mean pore diameter 60 Å was obtained from E. S. Industries (Marlton, N.J., U.S.A.) and a Partisil ODS 2 column (25 × 0.46 cm) packed with irregularly shaped 10-μm octadecyl–silica was obtained from Whatman (Clifton, N.J., U.S.A.). Bulk 5-μm Spherisorb ODS, a spherical octadecyl–silica with a mean pore diameter of 90° Å, was obtained from Phase Sep (Hauppage, N.Y., U.S.A.) and slurry packed to obtain 25 × 0.38 cm and 25 × 0.46 cm columns. Bulk 5- and 10-μm Partisil ODS were supplied by Whatman and packed into 25 × 0.46 cm columns from a slurry.

In all experiments with reversed-phase columns, the eluent was 50 mM phosphate buffer, pH 2.1. With the Chromegasorb column, n-hexane–chloroform mixtures were used. The solvents were "distilled in glass" materials from Burdick & Jackson

Labs. (Muskegon, Mich., U.S.A.). The chemicals were of reagent grade or of the highest available purity and were purchased from Fisher Scientific (Pittsburgh, Pa., U.S.A.) or Aldrich (Milwaukee, Wisc., U.S.A.).

The sample size was sufficiently small to avoid any overloading of the column. Sodium nitrate and tetrachloroethane were used as non-sorbed tracers with octadecyl–silica and silica columns, respectively. The distribution ratios, k', were calculated from the retention times of the tracers and eluites, which were evaluated at the maxima or from the center of gravity of the peaks. The k_0 values were calculated from the retention time of the tracer and the volumetric flow-rate of the eluent assuming a value of 0.4 for the interstitial porosity, ε_e, of the columns.

Chromatograms were recorded with Perkin-Elmer Model 56 strip-chart recorder as well as on floppy discs using a Model PDP 11/10 computer with an RX01 unit (Digital Equipment Corp., Maynard, Mass., U.S.A.). The AR11 analog–digital converter of the computer was connected to the detector via a home-built amplifier–high-frequency filter unit. The chromatograms were displayed on the screen of a VT55 Decscope (Digital Equipment Corp.), which also provided hard copies.

The variance of the chromatographic peaks was calculated from the peak width at half-height or by evaluating the second central moment of the peak fitted to a heterosemi-Gaussian distribution by the computer. The parameters of eqn. 26 were estimated by a weighted least-squares method. The programs were written in BASIC language. The above computer, with a Decwriter (Digital Equipment Corp.), was used to carry out all numerical calculations.

RESULTS AND DISCUSSION

The increasing use of column packed with microparticulate stationary phases for the separation of complex molecules in liquid chromatography both facilitates and necessitates further insight into the physico-chemical phenomena that govern band spreading and thereby significantly affect the efficiency of the chromatographic system.

Within the constraints of our model, the general plate height equation is believed to express accurately the plate height as a function of the various column and operational parameters. Eqn. 14 allows us to study the effect of these parameters on column efficiency over a wide range of flow velocities, provided that their values can be estimated. Plots of the reduced plate height against the reduced velocity for a very wide range of ν are shown in Fig. 6. The results were calculated by using the general plate height equation with values typical in modern liquid chromatography. In order to evaluate accurately all column parameters, it would be necessary to measure the plate height of various solutes with a given column without extra-column effects almost over the velocity span shown in Fig. 6. For practical reasons, this would be extremely difficult. In fact, in chromatographic practice, the reduced velocity range is small, as illustrated in Fig. 6, and the measurements that can safely be carried out with a single column are confined to an even narrower velocity range. Thus, the merit of the general plate height equation is to establish a quantitative relationship between the various factors involved in the band spreading process under the idealized conditions of the model.

Furthermore, eqn. 14 can be used to illustrate the effect of the various param-

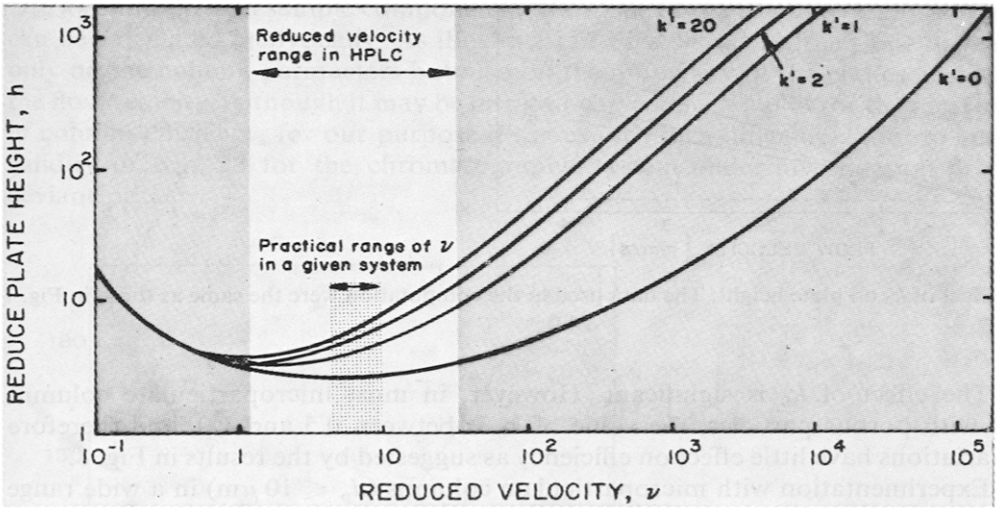

Fig. 6. Graph illustrating the reduced plate height as a function of the reduced velocity over a wide range of conditions according to the general plate height equation. The reduced velocity ranges encountered in common practice are also shown.

eters. Fig. 7 shows the plate height as a function of the flow velocity for different values of the distribution ratio. In Fig. 8 the effect of k_0, which is the ratio of the interparticular pore volume to the interstitial volume in the column, is depicted. In the calculation of the results presented in Figs. 7 and 8, values of the parameters typical in reversed-phase chromatography with 20–30-cm columns packed with 10-μm particles have been used. In practice, the plate height is often not such a strong function of the distribution ratio as shown in Fig. 7 because the experimentally measured plate height of early peaks is increased by extra-column band spreading. The quasi-linear plate height dependence on the flow velocity at the relatively high reduced velocities shown in Figs. 7 and 8 is frequently observed in practice. Nevertheless, the slope or intercept of these lines bears a very complex relationship to the actual column and operational parameters, and they therefore cannot be used to extract information required for the understanding of the actual chromatographic process and for column design from experimental data.

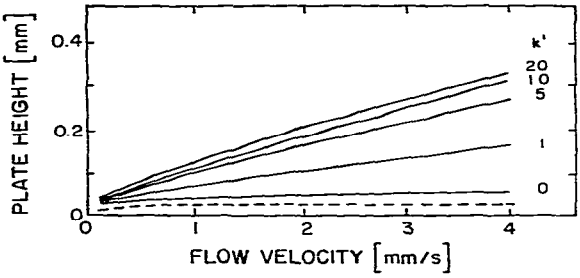

Fig. 7. Plate height as a function of the flow velocity with the distribution ratio as the parameter. The data used in the computation are as follows: $\gamma = 0.7$, $\lambda = 2.5$, $\omega = 2$, $\kappa = 1/15$, $k_0 = 0.8$, $\varepsilon_e = 0.4$, $\upsilon = 2$, $\varphi k_a/D_m = 1.25 \cdot 10^7\ \mathrm{cm}^{-2}$, $d_p = 10\ \mu\mathrm{m}$. The broken line illustrates the magnitude of H_{disp}.

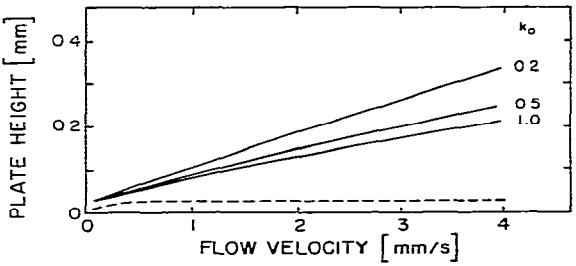

Fig. 8. Effect of k_0 on plate height. The data used in the computation were the same as those in Fig. 7 with $k' = 3$.

The effect of k_0 is significant. However, in most microparticulate columns packed with porous particles, the value of k_0 is between 0.5 and 1.0, and therefore small variations have little effect on efficiency as suggested by the results in Fig. 8.

Experimentation with microparticulate columns ($d_p \leqslant 10\,\mu m$) in a wide range of flow velocities is usually limited by the effect of extra-column band spreading at low velocities, the non-uniform radial temperature profile due to viscous dissipation and the pressure limitation of the instrument at high velocities. Consequently, it is desirable to estimate the individual plate height contributions from a set of experimental data obtained at flow velocities in the practical range.

The rearrangement of the general plate height equation with certain restrictions results in eqn. 26, which allows the calculation of $h_{disp.}$, $h_{kin.}$ and $h_{e.c.}$ with data measured, at least in principle, in a single chromatographic run, provided that the molecular dimensions, the diffusivity and the rate constant for the association step are about the same for all of the sample components. Although at least a five-component sample is needed, the intrinsic potential of chromatography to separate very closely related substances facilitates the selection of suitable sample components, *e.g.*, isomers. The requirements that the k_a values be close implies that the mechanism for the interaction between the eluites and the stationary phase is the same. Recent studies on reversed-phase chromatography suggest[11] that in this very important branch of modern liquid chromatography the mechanism of eluite binding is the same under widely ranging conditions. Unpublished results from our laboratory also show that the compensation temperature[12] is invariant in different reversed-phase systems.

In order to make use of eqn. 26, we have to calculate $h^0_{diff.}$ *a priori* from the interstitial flow velocity, the diffusivity of eluites, the mean particle diameter and the intra- and interparticulate void spaces in the column. These data are either available or can be measured. In addition, the numerical value of κ for mass transfer at the particle boundary as well as the tortuosity and configuration factors for $h_{i.eff.}$ are needed. In our calculations we used, on the basis of literature data, $\kappa = 1/15$ (ref. 13), $\theta = 2$ (ref. 14) and 1/30 for the configuration factor of spherical particles[1].

It is essential to establish that for the data obtained in a given chromatographic run the parameters a, b and c in eqn. 26 are indeed constant. Whereas the fit of the data to the parabolic equation can be tested by some of the usual statistical procedures, a simpler and more revealing approach is given by eqn. 33, which is applicable at sufficiently high k' values. Thus, a linear plot of the peak width against the distribution ratio can serve as a test for the validity of eqn. 26, *i.e.*, for the close similarity of

D_m, k_0 and k_a for all sample components. The slope of the asymptotically straight line can be calculated analytically. As illustrated in Figs. 9 and 10, the slope depends not only on the column parameters but also on the diffusivity of the eluites as well as on the flow velocity. Although it may be intriguing to use such a plot for the measurement of column efficiency, for our purpose it serves only as a diagnostic tool to verify the validity of eqn. 26 for the chromatographic system under investigation or to spot deviant peaks.

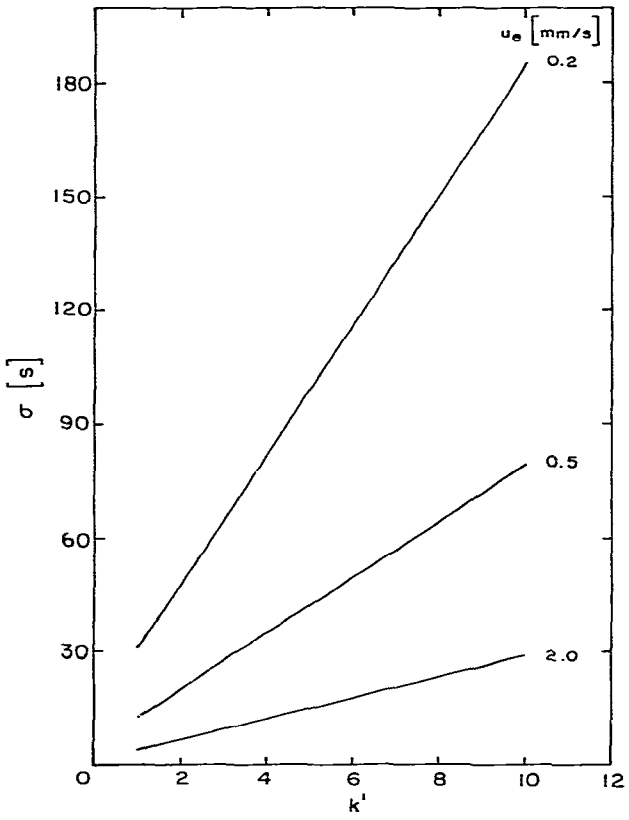

Fig. 9. Effect of flow velocity on the slope of the quasi-straight lines obtained by plotting the peak width against the distribution ratio. The data used in the calculation were the same as in Fig. 7 and D_m was assumed to be $2 \cdot 10^{-5}$ cm²/sec.

Fig. 11 shows a chromatogram of non-ionized aromatic acids obtained on an octadecyl–silica column with pure aqueous eluent together with the superimposed σ *versus* k' plot, which is linear. In the experiment, utmost care was taken to minimize extra-column band spreading. As can be seen in Table I, the diffusivities of the sample components are indeed commensurate. Figs. 12 and 13 illustrate chromatographic results obtained with an appropriate mixture of aromatic compounds on a silica gel column at different flow-rates of the *n*-hexane–chloroform mixture used as the eluent. The linear plot in Fig. 12 demonstrates that the individual plate height contributions

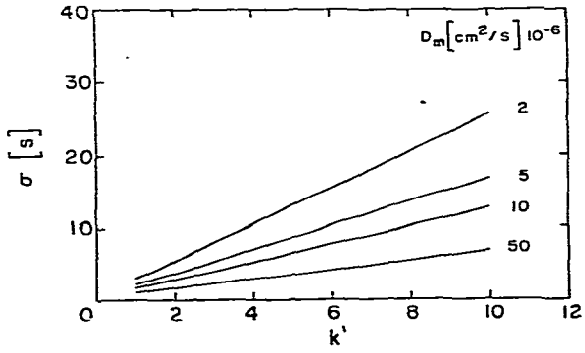

Fig. 10. Effect of diffusivity on the slope of the quasi-straight lines obtained by plotting the peak width against the distribution ratio. The results were calculated with the data used in Fig. 7 except $d_p = 5$ μm. The value of t_0 and L were taken as 50 sec and 25 cm, respectively.

can be evaluated by the use of eqn. 26 with this system also. Fig. 13 clearly shows the behavior of the plots at low k' values as predicted theoretically and illustrated schematically in Fig. 3.

In order to illustrate the effect of extra-column band spreading, experiments were carried out with a 5-μm Spherisorb ODS column whose outlet fitting had a large

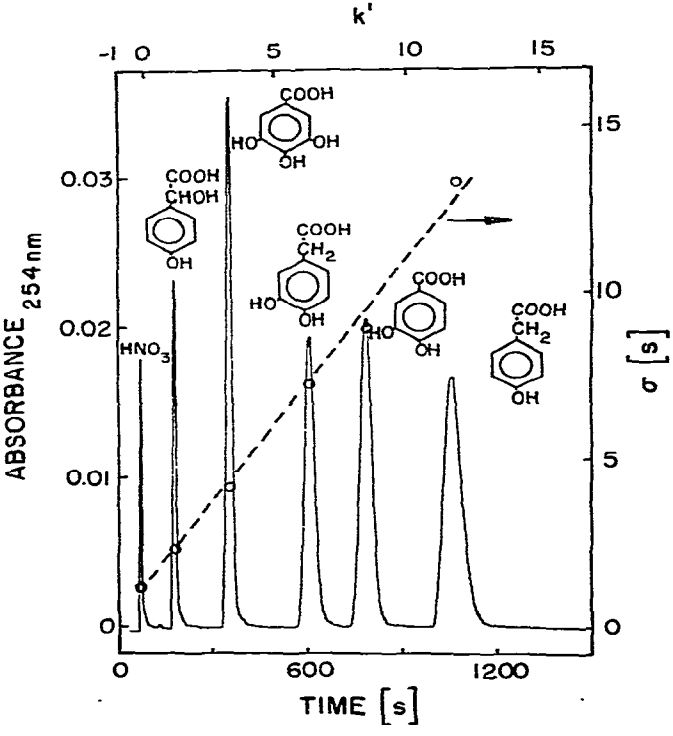

Fig. 11. Chromatogram of aromatic acids and plot of peak width against the distribution ratio. Column, 5-μm Spherisorb ODS, 25 × 0.38 cm; eluent, 50 mM phosphate buffer, pH 2.1; flow-rate, 3.0 ml/min; temperature, 23°; inlet pressure, 312 atm; UV detector.

TABLE I

DIFFUSION COEFFICIENTS IN WATER AT 23° CALCULATED BY THE WILKE–CHANG CORRELATION[9] FOR THE NON-IONIZED ELUITES SHOWN IN FIG. 11

k'	*Eluite*	*Diffusivity ($cm^2/sec \times 10^6$)*
1.4	4-Hydroxymandelic acid	6.59
3.6	2,3,4-Trihydroxybenzoic acid	6.59
6.9	3,4-Dihydroxyphenylacetic acid	6.59
9.2	3,5-Dihydroxybenzoic acid	7.11
12.6	4-Hydroxyphenylacetic acid	6.59

dead volume. The results in Fig. 14 show the expected curvature at low k' values. Such data sets, however, still could be analyzed by using eqn. 26, provided that there are a sufficient number of data points on the linear portion of the σ *versus* k' plot. Another type of curvature that is caused by significant differences in the D_m and/or k_a values for the sample components is illustrated in Fig. 15. The data were obtained by Halász *et al.*[15], who used a 7.5-cm column. With such a short column, extra-column band spreading may also be significant and affect the shape of curves at low k' values. Non-linear plots of the peak width against the distribution ratio such as those shown in Fig. 15 should serve as a caveat that the requirements for eqn. 26 to hold have not

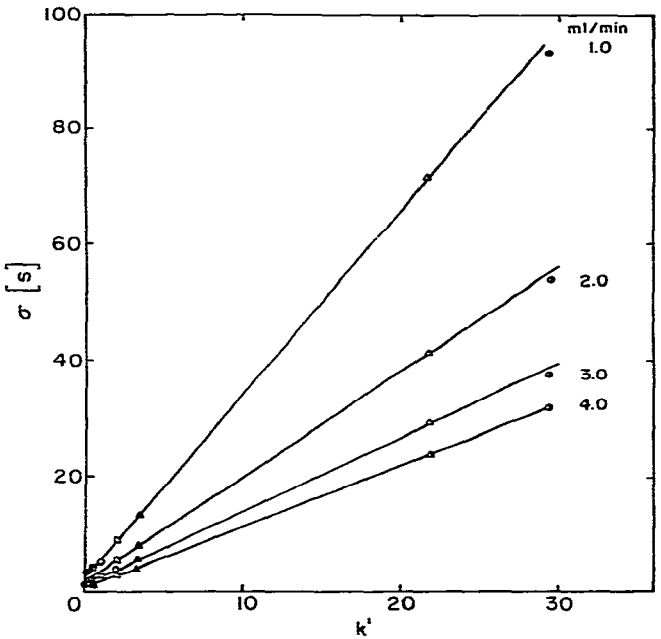

Fig. 12. Plot of the peak width, σ, against the distribution ratio, k', from chromatograms of aromatic compounds obtained with a silica gel column at different flow-rates. Column, 5-μm Chromegasorb R, 30 × 0.46 cm; eluent, *n*-hexane containing 5% (v/v) chloroform; temperature, 23°; UV detector at 254 nm. Sample components and diffusivities ($D_m \cdot 10^5$ cm^2/sec): *m*-xylene (3.02), α,α'-dichloro-*p*-xylene (2.62), nitrobenzene (3.25), benzaldehyde (3.00), acetophenone (3.17), α-naphthol (2.72) and phenol (3.49).

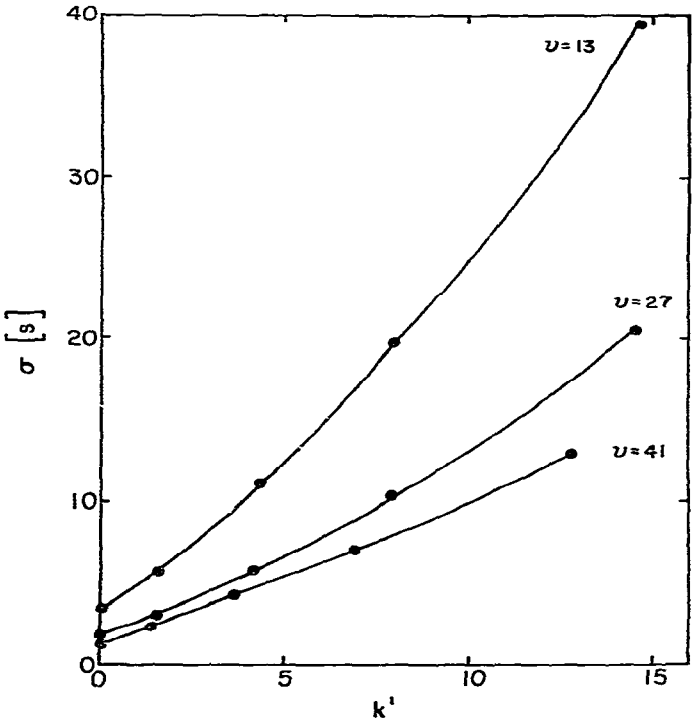

Fig. 13. Plot of the peak width, σ, against the distribution ratio, k', for aromatic acids from data obtained at various reduced velocities on a 5-μm Spherisorb ODS column under conditions stated in Fig. 11 except that the outlet fitting of the column had an intentionally large dead volume and 3,5-dihydroxybenzoic acid was not present in the sample.

been met and the method proposed for the analysis of such an experimental data set is precluded.

The plate height contributions have been evaluated by using the approach outlined in the theoretical section from experimental data obtained by using columns packed with silica or octadecyl–silica. As shown in Table II some of the columns were commercial products and others were packed in our laboratory with octadecyl–silica obtained from commercial sources. The operating conditions are also stated in Table II. The components of the sample mixtures were essentially the same as those which are shown in Figs. 11–14 for reversed-phase chromatography with pure aqueous eluent and for chromatography on silica gel with *n*-hexane–chloroform mixtures.

The plate heights and distribution ratios were evaluated and the parameters of eqn. 26 were calculated for each chromatographic run as described in the experimental section. At least three runs were made for a given set of conditions and average values were used for the calculations. The value of $H_{diff.}$ was calculated for each case by using eqns. 28 and 40. Then from the estimated parameters of the parabolic equation for $H_{eff.}$ the individual plate height contributions for a given solute under the conditions of the particular chromatographic run were calculated by using eqns. 37–39.

Typical results are shown in Table II. $H_{expt.}$ denotes the actually measured plate height, which is broken down into plate height increments attributed to the independent band spreading processes. The sum of these increments which arise from

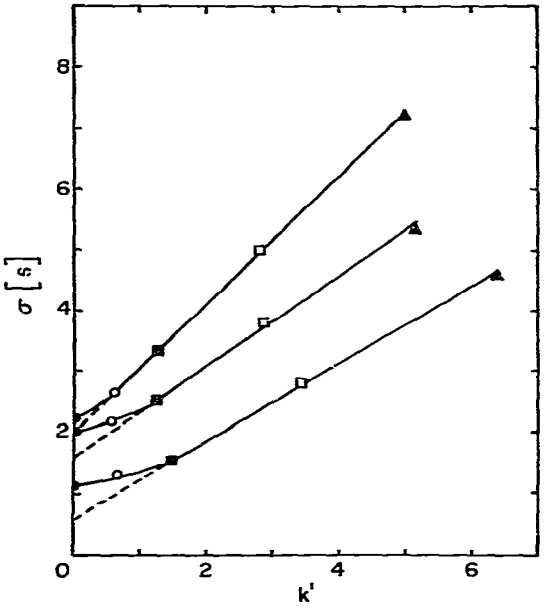

Fig. 14. Plot of σ against k' for the slightly retarded aromatic compounds separated on silica gel under the same conditions as shown in Fig. 12, except the eluent contained 5% (v/v) chloroform and the flow-rates were in the order of decreasing slope of the lines 2.0, 3.0 and 4.0 ml/min.

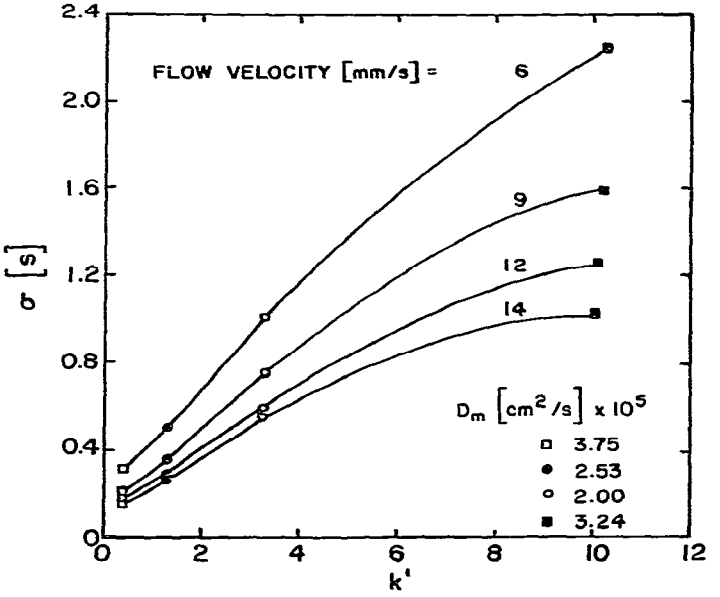

Fig. 15. Plot of the peak width, σ, against the distribution ratio, k', for a mixture whose components have significantly different diffusivities as illustrated. The data were obtained by Halász *et al.*[15] with aromatic compounds on a 7.5-cm silica gel column, $d_p = 4.2\ \mu$m, by using *n*-heptane as the eluent.

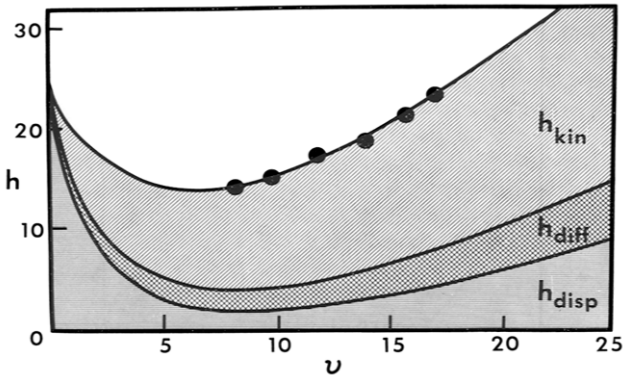

Fig. 16. Graph illustrating the magnitude of the individual plate height increments over a wide reduced velocity range as estimated from experimental data obtained with acetophenone on silica and shown by dots. Column, 5-μm Chromegasorb R, 30 × 0.46 cm; eluent, *n*-hexane with 10% (v/v) chloroform; temperature, 25°; UV detector at 254 nm.

phenomena inside the column is denoted by $H_{col.}$. Thus, the plate height contribution of extra-column band spreading is given by $H_{e.c.} = H_{expt.} - H_{col.}$

In all cases the effect of kinetic resistances which manifests itself in the magnitude of $H_{kin.}$ was found to be significant. It is noted that the 5-μm Partisil ODS

TABLE II

PLATE HEIGHT INCREMENTS EVALUATED FOR VARIOUS COLUMNS FROM EXPERIMENTS AT A SINGLE VELOCITY

Each chromatographic run was performed at least in triplicate. The diffusivities were calculated from the Wilke–Chang equation as $6.59 \cdot 10^{-6}$ (25°) and $11.17 \cdot 10^{-6}$ cm²/sec (50°) for gallic acid in water, $3.00 \cdot 10^{-5}$ cm²/sec for acetophenone and $3.49 \cdot 10^{-5}$ cm²/sec for phenol, both in *n*-hexane–chloroform (9:1). $H_{e.c.}$ denotes the plate height increment due to extra-column band spreading, $H_{col.}$ is the plate height calculated for the column proper and $H_{expt.}$ is the experimentally measured plate height.

Column	d_d (μm)	k_o	k'	$H_{disp.}$	$H_{diff.}$	$H_{kin.}$	$H_{col.}$ (μm)	$H_{e.c.}$	$H_{expt.}$	*Conditions**
Partisil ODS 2 (commercial)	10	0.6	5.7	173	18	33	224	0	224	a
Partisil ODS (home-packed)	5	0.6	3.6	356	5	24	385	0	385	a
Spherisorb ODS (home-packed)	5	0.9	4.1	17	5	59	81	3	84	b
Spherisorb ODS (home-packed)	5	0.9	1.9	2	3	15	20	2	22	c
Chromegasorb R (commercial)	5	0.88	3.4	34	3	32	69	5	74	d
Cromegasorb R (commercial)	5	0.88	29.0	34	4	50	88	0	88	e

* (a) Column, 25 × 0.46 cm I.D.; eluite, gallic acid; eluent, 50 m*M* phosphate buffer, pH 2.1; flow-rate, 2.0 ml/min; column inlet temperature, 25°. (b) As (a), but column I.D. 0.38 cm. (c) As (a), but column inlet temperature 50°. (d) Column, 30 × 0.46 cm I.D.; eluite, acetophenone; eluent, *n*-hexane–chloroform (9:1); flow-rate, 2.0 ml/min; column inlet temperature, 23°. (e) As (d), but with phenol as eluite.

column was packed by a procedure known to yield columns of poor efficiency, which explains the very high value of $H_{disp.}$. The commercial Partisil ODS 2 column had been used extensively prior to the experiments whose result is shown in Table II. It is conceivable that the packing of this column deteriorated with a concomitant increase in $H_{disp.}$. Columns packed with uniform spherical Spherisorb ODS particles show the lowest values of $H_{disp.}$. As the calculation of $H_{diff.}$ by eqn. 40 is expected to be the most reliable when the column material is spherical and has a uniform particle size distribution, the greatest accuracy in the values of the plate height increments is expected with the Spherisorb ODS column also. The results show that with these columns $H_{kin.}$ is the greatest contributor to the plate height attributed to the column only, $H_{col.}$. Extra-column band spreading was relatively unimportant in those experiments except when gallic acid was eluted at a low k' value in a chromatographic run at elevated temperature. The results with silica gel columns (Chromegasorb R) packed with irregularly shaped particles indicate again that the diffusional resistances have a minor effect and the plate height is essentially determined by $H_{disp.}$ and $H_{kin.}$.

The data presented in Table II include results obtained with columns which are considered by today's standards to be poor and/or acceptable. The calculated plate height contributions appear to reflect correctly the features of the individual column as well as the effect of the operating conditions.

Plate heights and plate height contributions calculated for the individual peaks on the chromatogram of an aromatic acid mixture are shown in Table III. The data were obtained with a column packed with 5-μm spherical octadecyl–silica particles by using neat aqueous phosphate buffer, pH 2.1, as the eluent. The pH was sufficiently low for the acids to be protonated. The results in Table III illustrate the effect of the distribution ratio on the measured plate height and the relative magnitude of the individual plate height increments. The value of the experimentally measured plate heights for early peaks is significantly influenced by the magnitude of $H_{e.c.}$, but the effect vanishes when the distribution ratio is sufficiently high. Of course, $H_{e.c.}$ could be further reduced by more careful experimental design, but the purpose of this study was also to obtain quantitative information on the magnitude of extra-column band spreading with an instrumental set-up and fittings frequently used in practice.

As seen from the low $H_{disp.}$ values, the column is well packed and axial dis-

TABLE III

EFFECT OF THE CAPACITY FACTOR ON THE VARIOUS PLATE HEIGHT CONTRIBUTIONS AT FIXED FLOW VELOCITY

Column, 5-μm Spherisorb ODS, 25 × 0.46 cm, home-packed; $k_0 = 0.9$; eluent, 50 mM phosphate buffer, pH 2.1; flow-rate, 2 ml/min; column inlet and wall temperature, 50°; inlet pressure, 166 atm. Each chromatographic run was performed at least in triplicate. See Table II for symbols. The diffusivities of the eluites are given in Tables I and IV.

Eluite	k'	$H_{disp.}$	$H_{diff.}$	$H_{kin.}$ (μm)	$H_{col.}$	$H_{e.c.}$	$H_{expt.}$
3,4-Dihydroxymandelic acid	0.50	1.9	1.7	3.8	7.5	7.5	15
4-Hydroxymandelic acid	0.95	1.9	2.2	8.3	12	4.5	16.5
2,3,4-Trihydroxybenzoic acid	1.87	1.9	2.7	15	20	2	22
3,4-Dihydroxyphenylacetic acid	3.88	1.9	3.3	22	27	0	27
4-Dihydroxyphenylacetic acid	7.19	1.9	3.6	27	33	0	33

persion in the interstitial space has a minor effect. The band spreading attributed to the column and measured by $H_{col.}$ is dominated by the plate height increment due to kinetic resistances, $H_{kin.}$, and the relative magnitude of this term rapidly increases with the distribution ratio. In contradistinction, $H_{diff.}$ is relatively small and a comparatively weak function of k'. We can conclude from the tabulated data that with a well packed microparticulate column and imperfect instrumentation, the broadening of early peaks is controlled by extra-column effects, whereas the plate height of strongly retarded peaks is dominated by the slowness of the binding kinetics at the stationary phase surface.

The effect of temperature on $H_{kin.}$ for aromatic acids has also been investigated by using a new commercial Partisil ODS 2 column and phosphate buffer, pH 2.1. The experiments were carried out in the temperature range 10–50° at 10° intervals. The standard enthalpy change for the reversible binding of the eluites by the stationary phase ligands, $\Delta H°$, was evaluated from Van 't Hoff plots. $H_{kin.}$ was evaluated for each eluite at five temperatures and the corresponding φk_a and k_d values were calculated by using eqn. 19. The phase ratio, φ, does not change appreciably in the temperature range investigated, and consequently the temperature dependence of φk_a is determined by that of k_a. Arrhenius plots for both φk_a and k_d yielded straight lines, from which the activation energies, E_a and E_d, for the rate of binding and dissociation, respectively, have been evaluated. The results are shown in Table IV. The $\Delta H°$ values are similar to those obtained with comparable reversed-phase systems[2]. The activation energy calculated for the binding step, E_a, commensurate with the activation energy of diffusivity, being of the order of 3 kcal/mole. On the other hand, the magnitude of the activation energy for the dissociation step, E_d, which is given by $E_a - \Delta H°$, is in the range typical of weak chemical interactions. As stated earlier, the kinetic model is crude so that the limited experimental data presented here do not allow us to draw conclusions as far as the mechanism of the binding process of such complicated molecules at the heterogeneous surface of the stationary phase is concerned. Nevertheless, we believe that there is sufficient evidence for the claim that kinetic resistances play a significant role in determining band spreading, particularly

TABLE IV

ENTHALPY OF BINDING AND ACTIVATION ENERGY OF THE RATE CONSTANTS IN REVERSED-PHASE CHROMATOGRAPHY OF ORGANIC ACIDS WITH PURE AQUEOUS ELUENT

Column, 5-μm Spherisorb ODS, 25 × 0.46 cm; eluent, 50 m*M* phosphate buffer, pH 2.1; flow-rate, 1.0 ml/min; temperature range, 10–50°. $\Delta H°$ is the standard enthalpy change for the eluite–stationary phase interaction; E_a and E_d are activation energies calculated for the rate of the association and dissociation processes, respectively. The diffusivities of the eluites in water at the different column temperatures were calculated by the Wilke–Chang correlation[9], (*cf.*, Table I). The diffusivity of 3,4-dihydroxymandelic acid at 23° is calculated as $6.43 \cdot 10^{-6}$ cm²/sec.

Eluite	*Range of k'*	$\Delta H°$	E_a *(kcal/mole)*	E_d *(kcal/mole)*
3,4-Dihydroxymandelic acid	0.61– 1.32	−3.48	3.31	6.79
4-Hydroxymandelic acid	1.21– 2.78	−3.76	3.31	7.07
3,4-Dihydroxyphenylacetic acid	4.68–15.92	−5.57	3.31	8.88
4-Hydroxyphenylacetic acid	8.95–31.53	−5.72	3.31	9.03

that of strongly retarded elutes in the microparticulate columns that are widely used in modern liquid chromatography.

Recent advances in the design of high-efficiency columns for liquid chromatography have been brought about by reducing the particle size of the stationary phase. It has been pointed out[15,16], however, that the pressure drop required to maintain a given flow velocity through the column increases rapidly with decreasing particle diameter and concomitantly the efficiency of the column is adversely affected by the "heat effect" due to viscous dissipation[17]. These observations led to the conclusion that in liquid chromatography there is a practical lower limit to the particle diameter which is in the range 1–3 μm (ref. 15) or 4–5 μm (ref. 16).

A major aim in deriving a general plate height equation and devising a method to factor out the individual plate height contributions has been the assessment of the effect of kinetic resistances on the efficiency of microparticulate columns. To our best knowledge, the problem has not been addressed in liquid chromatography although the excessive band spreading arising from the kinetics of adsorption on heterogeneous surfaces in gas chromatography has been investigated[1,18]. Experimental observations in our laboratory have indicated that with ionogenic eluites the slowness of attaining protonic equilibria in the mobile phase, which are generally assumed to take place "instantaneously", can cause undue band spreading and deformation of peak shape in high-performance columns. It follows that even if the kinetics of eluite binding at the stationary phase surface is fast by other standards, it may be sufficiently slow to affect adversely the dynamics of the chromatographic process in microparticulate columns that have high intrinsic efficiencies. In fact, kinetic resistances alone could set a practical lower limit to the particle diameter because it would be unreasonable to reduce the particle diameter beyond the point where $H_{\text{kin.}}$ becomes the largest plate height increment.

The data obtained in the course of this investigation allow us to calculate the ratio of $H_{\text{kin.}}$ to $H_{\text{diff.}}$ as a function of the particle diameter and typical results for eluites having different distribution ratios are illustrated in Fig. 17.

In the chromatographic system represented by the parameters given in the legend of Fig. 17, the two plate height contributions, $H_{\text{kin.}}$ and $H_{\text{diff.}}$, are about the same in the particle size range 5–10 μm. The rate constants used in this calculation are typical for reversed-phase chromatography with neat aqueous eluents and lower than those usually obtained on silica gel. Therefore, "kinetic control" of band spreading, arbitrarily defined by the k' dependent condition $H_{\text{kin.}} > H_{\text{diff.}}$, may occur at lower particle sizes in other systems. Of course, a more explicit definition of "kinetic control" can be given by $H_{\text{kin.}} > (H_{\text{disp.}} + H_{\text{diff.}})$, but this relationship depends on the column packing structure and the flow velocity as well.

As can be seen in Fig. 17, the ratio $H_{\text{kin.}}/H_{\text{diff.}}$ is very small for large particles so that under the conditions used in classical liquid chromatography kinetic resistances are likely to play a minor role in affecting band spreading. Fig. 17 also shows that the ratio $H_{\text{kin.}}/H_{\text{diff.}}$ increases with the distribution ratio. Thus, the effect of kinetic resistances is greater on the plate height of strongly retarded eluites than that of early peaks. This suggests that stepwise or gradient elution may be particularly advantageous with microparticulate columns.

The treatment of the chromatographic process in this paper is necessarily based on certain idealizations represented by the mathematical model. It has been assumed

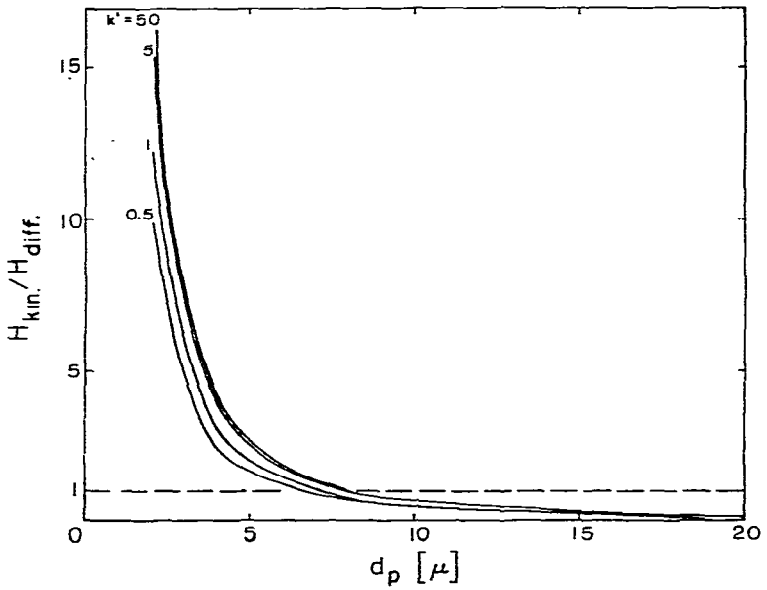

Fig. 17. Graph illustrating the dependence of the $H_{kin.}/H_{diff.}$ ratio on the particle diameter with k' as the parameter. The following data were used in the calculation: $\gamma = 0.7$, $\lambda = 2.5$, $\omega = 2$, $\kappa = 1/15$, $k_0 = 0.5$, $\theta = 2$, $D_m = 2 \cdot 10^{-5}$ cm²/sec, $u_e = 0.5$ cm/sec, $\varphi k_a = 2.5 \cdot 10^2$ sec^{-1}.

that the properties of the column are uniform or at least can be adequately described by the parameters which represent average values in real systems. For instance, no column material used in practice is truly monodisperse. Nevertheless, the use of an average particle diameter is permissible provided that the particle size distribution is sufficiently narrow.

The assumptions underlying the general plate equation, however, also include the introduction of the sample, as a very narrow plug, together with the eluent uniformly distributed over the column cross-section, the absence of "end-effects" at the inlet and outlet of the column and uniform column temperature. Whereas the effect of extra-column band spreading can be removed from the experimental values of plate height, the calculated plate height attributed to the column, $H_{col.}$, still may be influenced by the fact that some of the above assumptions do not hold rigorously. It is indeed unlikely that the assumptions apply fully to the conditions under which microparticulate columns are currently used in practice. With the commonly employed sampling valves, the eluent containing a slug of sample enters the column through a relatively narrow opening and in our experience the entrance conditions can have an effect on band spreading in short columns. Recently, Kirkland *et al.*[19] discussed the problems of sample introduction with regard to high-efficiency columns and demonstrated the importance of the entrance effect. Further studies are required, however, to establish the flow field at the column inlet and the spatial distribution of the eluite in the entrance region. In many practical situations the initial conditions can be non-ideal and contribute to the overall band spreading together with the flow field at the outlet, which is determined by the geometry of fittings and other appliances. In other words, the theory views the column as a piece of tubing containing a fixed bed of the stationary

phase proper, whereas in practice the end fittings, frits, etc., are also considered to be integral parts of the column.

When the particle size is small and the flow-rate is high, axial and radial temperature gradients are set up in the column due to the effect of viscous dissipation. As a non-uniform radial temperature profile augments band spreading, experimental results obtained with microparticulate columns can be strongly influenced by this phenomenon. In fact, the testing of the validity of the general plate height equation is impeded by the upper limit to the flow-rate at which the radial non-uniformity of temperature becomes appreciable in the column. By the use of narrow-bore columns, which played an important role at the beginning of modern liquid chromatography[20], the detrimental effect of viscous dissipation could be reduced. In such columns, a given linear flow velocity can be achieved at a relatively low volumetric flow-rate of the eluent due to the reduced cross-sectional area, and radial heat transfer is facilitated by the small tube radius.

Another deviation from ideal behavior can arise from the slow kinetics of certain secondary equilibria in the mobile phase. Although the resulting decrease in column efficiency and peak asymmetry is troublesome in practice, for the purpose of the measurements proposed in this study the effect can be avoided by selecting the chromatographic system carefully.

With all of these caveats, we believe that the approach outlined here can be used effectively to gain more insight into the column processes in liquid chromatography than is possible by conventional means. The results demonstrate that in microparticulate stationary phases the kinetics of the reversible binding of the eluite can affect the efficiency of the column. Despite the progress made in understanding the energetics of the binding process in reversed-phase chromatography[2], the mechanism of the interaction is far from understood. Consequently, any interpretation of rate constants obtained from chromatographic measurements requires further investigations into the detailed mechanism of the process in which solvation is likely to play an important role. Theoretical advances together with refinement of experimental techniques and data analysis may open the way for liquid chromatography to become a tool for physico-chemical measurements not only to gather thermodynamic information but also kinetic data.

ACKNOWLEDGEMENTS

This work was supported by grants GM20993 and CA21948 from the National Institutes of Health, DHEW. The authors are also indebted to The Gillette Company for financial support.

REFERENCES

1 J. C. Giddings, *Dynamics of Chromatography, Part I, Principles and Theory*, Marcel Dekker, New York, 1965.
2 C. Horváth, W. Melander and I. Molnár, *J. Chromatogr.*, 125 (1976) 129.
3 C. Horváth and H.-J. Lin, *J. Chromatogr.*, 126 (1976) 401.
4 O. Grubner, *Advan. Chromatogr.*, 6 (1968) 173.
5 J. F. K. Huber, *Ber. Bunsenges. Phys. Chem.*, 77 (1973) 179.
6 J. N. Done, G. J. Kennedy and J. H. Knox, in S. G. Perry and E. R. Adlard (Editors), *Gas Chromatography 1972*, Applied Science Publ., Barking, 1973, pp. 145–155.

7 R. Endele, I. Halász and K. Unger, *J. Chromatogr.*, 99 (1974) 377.
8 C. Horváth, in A. Zlatkis and L. Ettre (Editors), *Practice of Gas Chromatography*, Wiley, New York, 1967, pp. 129–238.
9 C. R. Wilke and P. Chang, *AIChEJ*, 1 (1955) 264.
10 M. J. E. Golay, *Anal. Chem.*, 40 (1968) 382.
11 C. Horváth, W. Melander and I. Molnár, *Anal. Chem.*, 49 (1977) 142.
12 R. Lumry and S. Rajender, *Biopolymers*, 9 (1970) 1125.
13 R. Pfeffer, *Ind. Eng. Chem. Fundam.*, 3 (1964) 380.
14 C. N. Satterfield, *Mass Transfer in Heterogeneous Catalysis*, MIT Press, Cambridge, Mass., 1970, p. 33.
15 I. Halász, R. Endele and J. Asshauer, *J. Chromatogr.*, 112 (1975) 37.
16 M. Martin, C. Eon and G. Guiochon, *J. Chromatogr.*, 99 (1974) 357.
17 H. L. Toor, *Ind. Eng. Chem. Process Des. Develop*, 48 (1956) 922.
18 J. Villermaux, *J. Chromatogr. Sci.*, 12 (1974) 822.
19 J. J. Kirkland, W. W. Yau, H. J. Stoklosa and C. H. Dilks, Jr., *J. Chromatogr. Sci.*, 15 (1977) 303.
20 C. Horváth, *Methods Biochem. Anal.*, 21 (1973) 79.